JOURNAL OF Applied Polymer SCIENCE

Non-Isothermal Degradation Kinetics of *N,N′*-Bismaleimide-4,4′-diphenylmethane/Barbituric Acid Based Polymers in the Presence of Hydroquinone

Quoc-Thai Pham,[1] Jung-Mu Hsu,[2] Jing-Pin Pan,[2] Tsung-Hsiung Wang,[2] Chorng-Shyan Chern[1]

[1]Department of Chemical Engineering, National Taiwan University of Science and Technology, Taipei 106, Taiwan

[2]Materials and Chemical Research Laboratories, Industrial Technology Research Institute, Chutung, Hsinchu 31015, Taiwan

Correspondence to: C. S. Chern (E-mail: cschern@mail.ntust.edu.tw)

ABSTRACT: The non-isothermal degradation kinetics of the cured polymer samples of *N,N′*-bismaleimide-4,4′-diphenylmethane/barbituric acid [BMI/BTA = 2/1 (mol/mol)] based polymers in the presence of hydroquinone (HQ) and native BMI/BTA was investigated by the thermogravimetric (TG) technique. By adding 5 wt % HQ into the BMI/BTA polymerization, the activation energy (E_a) of the thermal degradation process increased significantly in comparison with native BMI/BTA. Thus, the thermal stability of the cured polymer sample in the presence of HQ was greatly improved. The thermal degradation process exhibits three distinct stages. The key kinetic parameters associated with these stages were attained via the model-fitting method. For the sample of native BMI/BTA, the thermal degradation process was primarily controlled by nucleation, followed by the multi-decay law in the first stage. In contrast, the reaction order model adequately described the thermal degradation kinetics in the second stage. As to the last stage, the complex processes were described satisfactorily by the best-fitted reaction model. For the sample of BMI/BTA/5 wt % HQ, the degradation process was controlled by the nucleation mechanism, followed by the multi-molecular decay law in the first stage. In contrast, the second stage was controlled by the mixed mode of the competitive reaction order mechanism and 3-D diffusion mechanism. In the third stage, the complex processes were also adequately described by the best-fitted reaction model. All the experimental results illustrated that incorporation of 5 wt % HQ into the BMI/BTA based polymer resulted in the best thermal stability. © 2013 Wiley Periodicals, Inc. J. Appl. Polym. Sci. 130: 1923–1930, 2013

KEYWORDS: degradation; kinetics; thermal properties; dendrimers; hyperbranched polymers and macrocycles; polyimides

Received 21 January 2013; accepted 3 April 2013; Published online 10 May 2013

DOI: 10.1002/app.39360

INTRODUCTION

N,N′-Bismaleimide-4,4′-diphenylmethane (BMI) based polymers exhibiting a hyper-branched or highly cross-linked network structure (depending on the extent of conversion) offer excellent mechanical properties, chemical resistance, thermal stability, and attractive cost/performance ratio. As a result, these polymeric products have been widely used in many applications such as aerospace and electronics industries. With the reactive bismaleimide groups (two terminal −C=C− groups), BMI can polymerize with active hydrogen atom-containing species such as multi-amines and barbituric acid (BTA) via the Michael addition reaction mechanism.[1–6] It can also polymerize via the free radical polymerization mechanism using barbituric acid (BTA) or 2,2′-azobisisobutyronitrile (AIBN) as the thermal initiator.[7–10] Furthermore, anionic polymerization of BMI can be initiated by nano-Na^+/TiO_2.[11] In our recent study,[10,12] it was illustrated that Michael addition and free radical polymerization mechanisms competed with each other in the polymerizations of BMI with BTA in the temperature range 100–130°C (Scheme 1). The contribution of the free radical polymerization mechanism to the reaction of BMI with BTA increased with decreasing the mole fraction of BTA in the reaction medium.

Recently, hydroquinone (HQ) was used to effectively inhibit the free radical polymerization of BMI with BTA. In this manner, the sole Michael addition polymerization kinetics for the reaction system of BMI/BTA [2/1 (mol/mol)] in the presence of HQ was successfully investigated.[10,13] It was shown that the key kinetic parameters [e.g., reaction order, reaction rate constants, and activation energy (E_a)] of the Michael addition polymerization of BMI/BTA in presence of HQ were quite different from those obtained from the polymerization of BMI with BTA exhibiting the mixed mode of competitive free radical and Michael addition polymerization mechanisms.[13] The polymeric materials prepared by the polymerizations of BMI with BTA

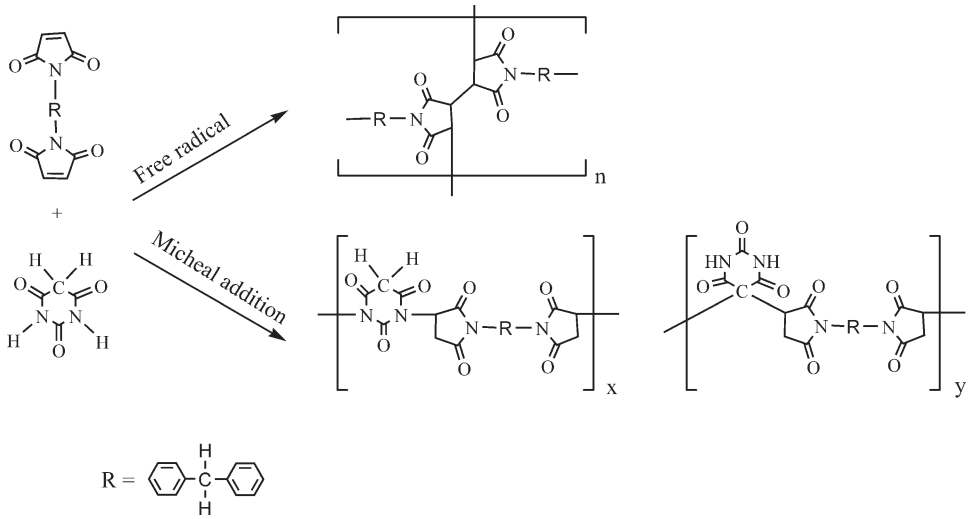

Scheme 1. Schematic representation of the free radical and Michael addition polymerization mechanisms for the reaction of BMI with BTA.

with and without HQ are expected to show different physicochemical properties. It is noteworthy that the BMI/BTA-based polymers exhibit very high glass transition temperature and excellent heat resistance that have a potential use in the design of lithium-ions batteries, where heat resistance is a crucial safety issue.[12] A semi-crystalline polymeric film (termed as the separator) such as polyethylene and polypropylene with a melting point of *ca.* 110–140°C is generally used to prevent short circuiting. Incorporating a small amount of BMI/BTA-based polymers into lithium-ions batteries provides a second protection mechanism functioning at around 200–230°C that suppresses the disastrous thermal run away (>700°C) that would ultimately lead to an explosion. Thus, the objective of this work was to investigate the non-isothermal degradation kinetics of the cured samples of native BMI/BTA [2/1 (mol/mol)] and BMI/BTA in the presence of HQ in solid state in order to gain a fundamental understanding of the thermal degradation process and mechanism.

EXPERIMENTAL

Materials

The chemicals used in this study include *N,N′*-bismaleimide-4,4′-diphenylmethane (95%, Beil), barbituric acid (99+%, ACROS), hydroquinone (99%, ACROS), and *N*-methyl-2-pyrrolidone (99%, ACROS). All chemicals are reagent grade and used as received.

Preparation of Samples

The polymerization of BMI/BTA [2/1 (mol/mol)] in NMP was carried out in a sealed 20-mL glass vial with magnetic mixing at 80°C over a period of 2 h in the absence of HQ or in the presence of HQ (5 wt % based on total solids content). The total solids content was kept constant at 20 wt % throughout this study. The reaction temperature was controlled by immersing the reactor in a thermostatic water bath. The sample obtained from the polymerization of BMI with BTA in the presence of 5 wt % was denoted as S5.

In our previous study,[15] the DSC curve showed a broad exothermic peak in the temperature range 100–280°C for the uncured sample of the BMI/BTA oligomer, which was attributed to the further polymerization of the residual reactive groups. Thus, before polymer characterization, the uncured samples of the native BMI/BTA and S5 oligomers were cured at 130°C for 6 h, post-cured in a vacuum oven at 200°C for 18 h, and finally in TG instrument at 250°C for 1 h to eliminate the residual solvent and moisture (if present).

Characterization

The kinetic parameters of the thermal degradation process including the activation energy (E_a), pre-exponential factor (A), and reaction model $f(\alpha)$ were determined by the thermogravimetric (TG) technique.[14–18] The characteristic weight loss data were recorded on the Diamond TG/DTA instrument (Perkin Elmer) in the temperature range 200–800°C under a nitrogen flow rate of 20 mL min^{-1}. The distance between two adjacent data points of weight percentage in the TG profile is 1 s (Δt = 1 s). The sample weight of 6.5 ± 0.2 mg was used in this study.

Determination of Kinetic Parameters

The thermal degradation rate ($d\alpha/dt$) of the single-step degradation reaction can be described by the following equation:

$$d\alpha/dt = A[\exp(-E_a/RT)]f(\alpha) \quad (1)$$

where α, defined by eq. (2), is the fractional conversion, t is time, R is the gas constant, and T is the absolute temperature.

$$\alpha = (m_0 - m_T)/(m_0 - m_f) \quad (2)$$

where m_0 is the initial weight percentage (100%), m_T is the weight percentage at temperature T, and m_f is the weight percentage at the final temperature. Typical ideal reaction models [$f(\alpha)$] reported in the literature can be expressed as follows[14,19]:

$$f(\alpha) = c(1-\alpha)^n \alpha^m \quad (3)$$

where m, n, and c are adjustable parameters. Some representative ideal reaction models [$f(\alpha)$] with the characteristic values of m, n, and c and their corresponding equivalent Sestak–Berggren

Table I. Some Representative Ideal Kinetic Models [$f(\alpha)$] Commonly Used in Solid State Degradation Reactions and Their Corresponding Equivalent Sestak–Berggren Reduced Equations

Mechanism	Code	$f(\alpha)$	Parameters of $f(\alpha)$: $c(1-\alpha)^n\alpha^m$
Nucleation models			
Random instant nucleation and two-dimensional growth of nuclei (Avrami–Erofeyev equation)	A2	$2(1-\alpha)[-\ln(1-\alpha)]^{1/2}$	$2.079(1-\alpha)^{0.806}\ \alpha^{0.515}$
Random instant nucleation and three-dimensional growth of nuclei (Avrami–Erofeyev equation)	A3	$3(1-\alpha)[-\ln(1-\alpha)]^{2/3}$	$3.192(1-\alpha)^{0.748}\ \alpha^{0.693}$
Geometrical contraction models			
Phase boundary controlled reaction (contracting area, i.e., bidimensional shape)	R2	$(1-\alpha)^{1/2}$	$(1-\alpha)^{1/2}$
Phase boundary controlled reaction (contracting volume, i.e., tridimensional shape)	R3	$(1-\alpha)^{2/3}$	$(1-\alpha)^{2/3}$
Reaction order models			
Unimolecular decay law (instantaneous nucleation and unidimensional growth)	F1	$(1-\alpha)$	$(1-\alpha)$
Multi-molecular decay law	Fn	$(1-\alpha)^n$	$(1-\alpha)^n$
Diffusion models			
One-dimensional diffusion	D1	α^{-1}	α^{-1}
Two-dimensional diffusion (bidimensional particle shape)	D2	$[-\ln(1-\alpha)]^{-1}$	$0.973(1-\alpha)^{0.425}\ \alpha^{-1.008}$
Three-dimensional diffusion (tridimensional particle shape) Jander equation	D3	$\frac{3(1-\alpha)^{2/3}}{2\left(1-(1-\alpha)^{1/3}\right)}$	$4.431(1-\alpha)^{0.951}\ \alpha^{-1.004}$

reduced equations are summarized in Table I.[19–22] For a non-isothermal thermal degradation process, the temperature is varied by a constant heating rate β ($\beta = dT/dt$) and α can be analyzed according to the following equation:

$$\begin{aligned} d\alpha/dt &= \beta(d\alpha/dT) \\ &= A[\exp(-E_a/RT)]f(\alpha) \end{aligned} \quad (4)$$

There are two common methods available for the analysis of thermal degradation kinetics, that is, the model-free and model-fitting methods. The model-free method is independent of reaction models and, consequently, it can be used to calculate E_a without resort to any model assumption. On the other hand, based on the model-fitting method, the kinetic parameters including E_a, $f(\alpha)$, and A are required to describe the complete thermal degradation kinetics. Equations ((5)) and ((6)) are defined for the model-free and model-fitting methods, respectively, as follows.[19,20]

$$\begin{aligned} \ln(d\alpha/dt) &= \ln(\beta\, d\alpha/dT) \\ &= -E_a/RT + \ln[Af(\alpha)] \end{aligned} \quad (5)$$

$$\begin{aligned} \ln[(d\alpha/dt)/(1-\alpha)^n\alpha^m] &= \ln[(\beta\, d\alpha/dT)(1-\alpha)^n\alpha^m] \\ &= -E_a/RT + \ln(cA) \end{aligned} \quad (6)$$

According to eq. (5) (Friedman method), E_a and ln [$A\ f(\alpha)$] at each α of different β values can be obtained from the least-squares best-fitted slope and intercept of the ln ($d\alpha/dt$) versus $1/T$ data, respectively. In contrast, the key kinetic parameters can be obtained from eq. (6). For example, plotting the ln [$(d\alpha/dt)/(1-\alpha)^n\alpha^m$] versus $1/T$ data should result in a straight line with the best fitted values of the parameter. The linearity is evaluated by the coefficient of determination (R^2) and the maximum value of R^2 is identified through adjustable processes of the parameters n and m. In this manner, the slope and intercept of the straight line represent the values of $-E_a/R$ and ln(cA), respectively. It should be noted that the E_a data obtained from the model-free method is used as the reference herein. That is, to be self-consistent throughout this study, the values of E_a obtained from the model-fitting method should be close to the average of E_a determined by the model-free method.

RESULTS AND DISCUSSION

Thermal Properties

The TG data are summarized in Table II. For example, the thermal degradation temperatures at which 10% weight loss ($T_{10\%}$) takes place at $\beta = 5°C\ min^{-1}$ for the cured polymer samples of native BMI/BTA and S5 are 356.5 and 369.1°C, respectively. In addition, all the values of $T_{2\%}$, $T_{5\%}$, $T_{10\%}$, $T_{20\%}$, $T_{40\%}$, and residue at 800°C for the cured sample of S5 are higher than those of native BMI/BTA. All these results indicate that incorporation of 5 wt % HQ into the BMI/BTA polymerization system greatly enhances its thermal stability.

Thermal Degradation Kinetics

Determination of E_a from the Model-Free Method. The representative TG data and the corresponding plots of $d\alpha/dt$ versus α for the cured polymer samples of native BMI/BTA and BMI/BTA in the presence of 5 wt % HQ (S5) at $\beta = 3$, 5, 10, and $20°C\ min^{-1}$ are shown in Figure 1. The model-free method was used to determine E_a at constant α in the α range 0.05–0.9 for the cured polymer samples of the pristine BMI/BTA and S5,

Table II. Characteristic Thermal Degradation Data Obtained from TG Experiments at $\beta = 5°C\ min^{-1}$ for the Cured Samples of Native BMI/BTA and S5

	T (°C)					
Sample	2% weight loss	5% weight loss	10% weight loss	20% weight loss	40% weight loss	Residue at 800 (°C) (%)
Native BMI/BTA	314.8	334.7	356.5	433.3	529.5	47.2
S5	326.2	347.2	369.1	441	551.7	49.7

since E_a for $\alpha < 0.05$ and $\alpha > 0.9$ can be affected strongly by possible minor errors in baseline determination.[14] The model-free approach [eq. (5)] was used to determine E_a at constant α. According to eq. (5), plotting $\ln(d\alpha/dt)$ versus $1/T$ for the TG experiments with different heating rates should result in a straight line with a slope equal to $-E_a/R$ at each α. The E_a data as a function of α for the cured polymer samples of native BMI/BTA and S5 thus obtained are shown in Figure 2. Note that there are three major degradation stages observed in the non-isothermal degradation process, as illustrated in the $d\alpha/dt$ versus α for the cured polymer samples of native BMI/BTA [Figure 1(b)] and S5 [Figure 1(d)]. However, there is also some overlap between two adjacent degradation stages. Taking the TG experiment of the cured sample of native BMI/BTA with $\beta = 5°C\ min^{-1}$ as an example, the first stage occurred in the α range 0.05–0.25 (or in the corresponding temperature range 320–380°C), the second stage took place in the α range 0.3–0.55 (or in the corresponding temperature range 408–461°C), and the third stage occurred in the range α 0.6–0.9 (or in the corresponding temperature range 474–583°C) as shown by the solid curve in Figure (1b). In Figure 2, the relatively constant E_a values of the cured polymer sample of native BMI/BTA are obtained in the α range 0.05–0.2 ($E_a = 214.26 \pm 4.43$ kJ mol^{-1}), 0.3–0.55 ($E_a = 347.88 \pm 3.05$ kJ mol^{-1}), and 0.65–0.85 ($E_a = 336.12 \pm 5.53$ kJ mol^{-1}). This result implies that the overlapping region between the first stage and the second stage occurs around the α range 0.2–0.3, and that between the second stage and the third stage around the α range 0.55–0.65. These

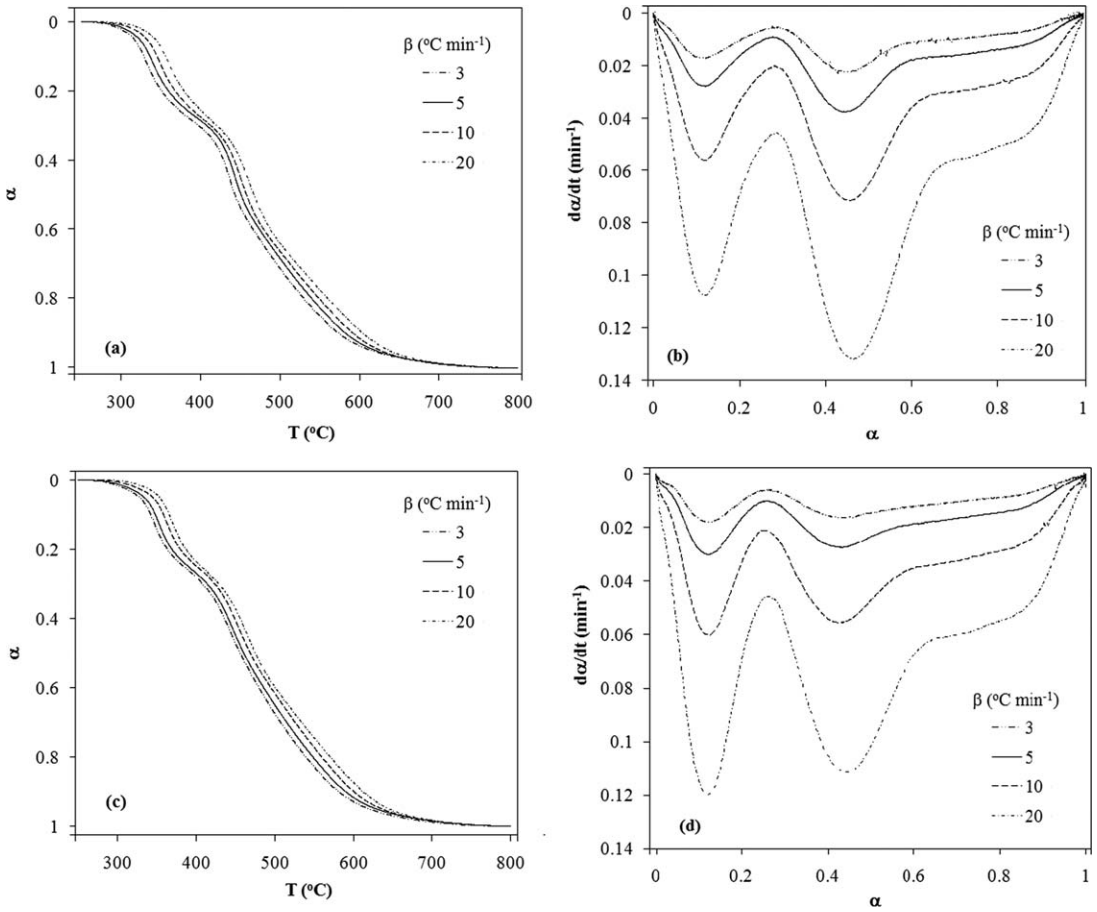

Figure 1. Representative plots of α versus T and $d\alpha/dt$ versus α at four different heating rates for the cured polymer samples of (a, b) native BMI/BTA and (c, d) S5.

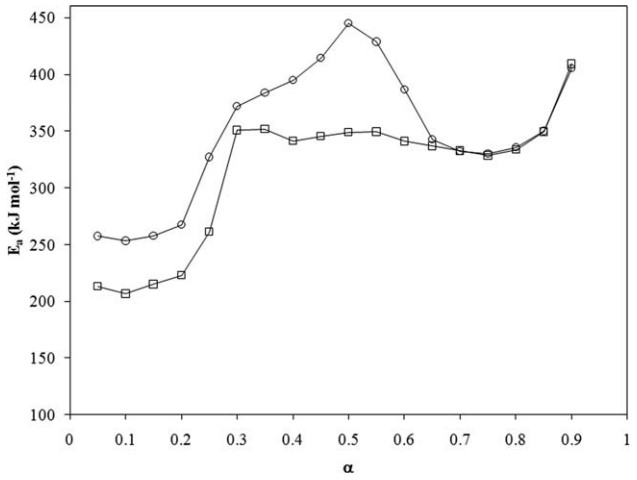

Figure 2. E_a versus α data for the cured polymer sample of (□) native BMI/BTA and (○) S5 obtained from the model-free method.

E_a data also show that the thermal degradation process is a single-step reaction (i.e., invariant activation energy) in each distinct stage.[14,23] Beyond stage 3 ($\alpha > 0.85$) thermal degradation kinetic is not a major concern in this study and will not be further discussed herein. As to the cured polymer sample of S5, the relatively constant E_a values are also observed in the α range 0.05–0.2 (Stage 1, E_a = 257.23 ± 4.44 kJ mol^{-1}) and in the α range 0.6–0.85 (Stage 3, E_a = 337.23 ± 6.68 kJ mol^{-1}). In contrast, the increased E_a value with α is observed in the α range 0.3–0.5 (Stage 2, E_a = 371.82–445.16 kJ mol^{-1}), which is most likely due to the multiple-step reaction.[23]

The profiles of the E_a versus α data for the cured polymer samples of native BMI/BTA and S5 are shown in Figure 2. It is shown that the E_a value of the cured sample of S5 is higher than that of native BMI/BTA in the α range 0.05–0.6, whereas the difference in E_a becomes insignificant beyond the α value of 0.6. In addition to the determination of E_a, the degradation rate constants for the cured polymer sample of native BMI/BTA and S5 at 350°C (in the first stage) were also calculated to be 0.0331 and 0.0168 min^{-1}, respectively, based on the model-free method. Base on the kinetic parameters (E_a and A) determined by the model-free method, it can be concluded that incorporation of a small quantity (e.g., 5 wt % used in this study) of HQ into the BMI/BTA polymer greatly enhances its thermal stability. This is most likely due to the fact that the presence of an adequate level of HQ can effectively suppress the free radical polymerization of the two carbon–carbon double bonds of BMI initiated by BTA. Thus, only the mechanism of the Michael addition polymerization between the two −C=C− groups of BMI and the active hydrogen atoms of the $>CH_2$ and >NH groups of BTA is operated in the reaction system of BMI/BTA in the presence of 5 wt % HQ. In contrast, Michael addition and free radical polymerization mechanisms competed with each other in the polymerization system of BMI/BTA in the absence of HQ (Scheme 1). Detailed mechanisms about the polymerization of BMI with BTA are explained in our previous articles.[10,12,13] As a consequence, the cured polymer samples of native BMI/BTA and S5 are expected to possess different molecular structures. Under the circumstance, the thermal degradation mechanism and the relevant kinetic parameters of the cured polymer sample of S5 are quite different from those of the counterpart of native BMI/BTA.

Determination of Kinetic Parameters from the Model-Fitting Method. In general, the deconvolution technique is very effective in the kinetic analysis of complex thermal degradation reactions involving simultaneous overlapping processes. However, we have tried every effort to use such a technique in combination with a variety of functions available in the Peakfit (Systat Software) to fit the individual peaks in the DTG curves via the nonlinear best-fitting method in this study, but eventually unsuccessful. This is probably because the DTG data in the second stage are severely overlaid with those in both the first and third stages for the cured polymer samples of native BMI/BTA and S5 [Figure 1(b,d)]. Furthermore, there are at least two simultaneous processes occurring in the second stage for the cured polymer sample of S5, as illustrated by the increased E_a with α in the α range 0.3–0.5 (Figure 2, the circular data points). The kinetic parameters of the three distinct stages should be determined in the α range without overlap to avoid the interference of the adjacent stage. As aforementioned, eq. (6) in combination with the $\ln[(d\alpha/dt)/(1-\alpha)^n\alpha^m]$ versus $1/T$ data can be used to simultaneously determine the kinetic parameters [E_a, cA, and (n, m)] by the optimization procedure of n and m.

Representative plots of $\ln[(d\alpha/dt)/(1-\alpha)^n\alpha^m]$ versus $1/T$ at β = 5°C min^{-1} for the three distinct stages of the thermal degradation process for the cured polymer samples of BMI/BTA is shown in Figure 3. For the purpose of better illustration, the original continuous $\ln[(d\alpha/dt)/(1-\alpha)^n\alpha^m]$ versus $1/T$ curves (experimental data) are represented by the discrete data points. In contrast, the solid straight lines represent the calculated results of the best reaction models. The E_a and cA parameters thus obtained from the model-fitting method for the first stage (α = 0.05–0.20) of the cured polymer sample of native BMI/BTA at β = 5°C min^{-1} are 211.03 kJ mol^{-1} and 1.20 × 10^{17} min^{-1},

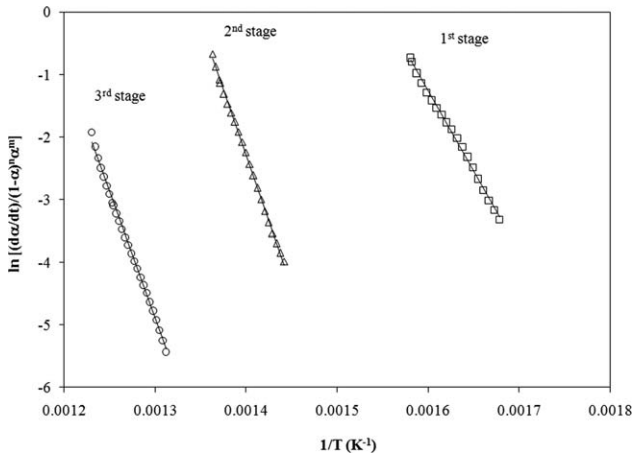

Figure 3. Representative plots of $\ln[(d\alpha/dt)/(1-\alpha)^n\alpha^m]$ versus $1/T$ for the three distinct stages of the thermal degradation process for the cured polymer samples of native BMI/BTA. The discrete data points represent the TG experimental data, and the continuous line the least-squares best-fitted straight line according to eq. (6).

Applied Polymer SCIENCE

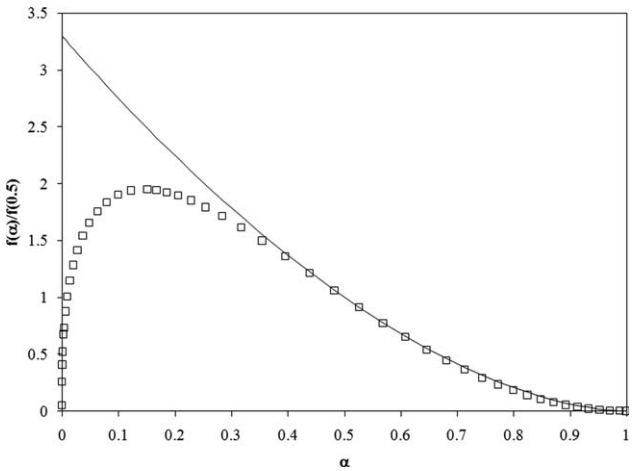

Figure 4. Comparison of $f(\alpha)$ normalized at $\alpha = 0.5$ $[f(\alpha)/f(0.5)]$ in the first stage determined by the model-fitting method with different sets of n and m values for the cured polymer sample of native BMI/BTA: the least-squares best-fitted model with $n = 2.05$ and $m = 0.35$ (the discrete data points); the reference model with $n = 1.72$ and $m = 0$ (the continuous line). Note that $\alpha = 0$ in the abscissae represents the start of the first stage and $\alpha = 1$ represents the end of the first stage.

respectively, with the highest R^2 of 0.997 for $n = 2.05$ and $m = 0.35$. This indicates that the thermal degradation mechanism of the first stage is controlled by nucleation followed by the linear growth of nuclei and the later progressing stage when $n > 1$ and $m < 1$.[22] The thermal degradation process can occur as follows: (a) instantaneous chain growth of nuclei including the possibility of their branching, (b) fast in interaction of branching nuclei interacting during their growth, and (c) later slowly progressing stage of (a) and (b).[22] It should be noted that the best mechanism chosen for predicting the thermal degradation kinetics will be transformed from the reaction order models to nucleation models when the parameter m increases from zero to a value greater than 0.5 (Table I). In the optimization of the parameters n and m, increasing n will result in an increase in E_a, whereas, increasing m will then lead to a reduction in E_a. In order to gain a better understanding of the thermal degradation mechanism involved in the first stage for the cured polymer sample of native BMI/BTA, the reaction order model (i.e., $m = 0$) was taken as the reference. It should be note that the corresponding E_a obtained from the reference model should be very close to the E_a value (211.03 kJ mol^{-1}) obtained from the above least-squares best-fitted model ($n = 2.05$ and $m = 0.35$). In this manner, the optimal value of $n = 1.72$ and $m = 0$ ($R^2 = 0.988$, a quite poor fit) were achieved, and the corresponding values of E_a and cA equal to 214.07 kJ mol^{-1} and 1.29×10^{17} min^{-1}, respectively. The model $f(\alpha)$ normalized at $\alpha = 0.5$ $[f(\alpha)/f(0.5)]$ with $n = 2.05$ and $m = 0.35$ (discrete data points) and the reference model with $n = 1.72$ and $m = 0$ (solid line) are shown in Figure 4. The values of n (1.72) and m (0) associated with the reference model indicate that it is the multi-molecular decay law that predominates in the first stage of the thermal degradation process for the cured polymer sample of native BMI/BTA.[24] The significant deviation between the least-squares best-fitted model ($n = 2.05$ and $m = 0.35$, the discrete data points in Figure 4) and the reference model (the continuous line in Figure 4) in the α range 0–0.35 in the first stage strongly suggest that the thermal degradation process can be described by the nucleation mechanism during the early stage 1,[22] followed by the multi-molecular decay law beyond a α value of 0.35 in the first stage.[19]

For the second stage, the optimal value of $n = 1.75$ and $m = 0$ with the highest value of R^2 (0.999) and the corresponding values of E_a and cA equal to 348.60 kJ mol^{-1} and 3.09×10^{24} min^{-1}, respectively, are obtained for the second stage ($\alpha = 0.35$–0.55). This result verifies that all the branching nuclei were degraded in the first stage. This was followed by the degradation of the part of the BMI/BTA crosslinked network structure with a relatively high crosslinking density in the second stage controlled by the multi-molecular decay law.[19] For the third stage ($\alpha = 0.65$–0.85), the kinetic parameters obtained from the optimization procedure for the $\ln[(d\alpha/dt)/(1-\alpha)^n\alpha^m]$ versus $1/T$ data are $n = 1.65$, $m = -1.005$, $E_a = 336.00$ kJ mol^{-1}, and $cA = 5.04 \times 10^{20}$ with R^2 (0.998). The profile of $f(\alpha)/f(\alpha = 0.5)$ calculated by using the values of $n = 1.65$ and $m = -1.005$ is shown in by the dashed line Figure 5 to be compared with some of the ideal kinetic models. It is shown that even though the model obtained from the third stage ($n = 1.65$ and $m = -1.005$) does not match any ideal models (Table I), it is the closest to the 3-D diffusion model (corresponding to $n = 0.951$ and $m = -1.004$). In addition, the E_a value obtained from the model-fitting method for the third stage of the cured polymer sample of native BMI/BTA at $\beta = 5$°C min^{-1} is 240 kJ mol^{-1}, with the coefficient of determination ($R^2 = 0.997$) for the 3-D diffusion model (corresponding to $n = 0.951$ and $m = -1.004$). It should be noted that the E_a value obtained from the model-fitting method with the 3-D diffusion model is also the highest compared to some of the other ideal models. However, this 3-D diffusion model is not suitably because its E_a (240 kJ mol^{-1}) obtained from model-fitting method is much lower

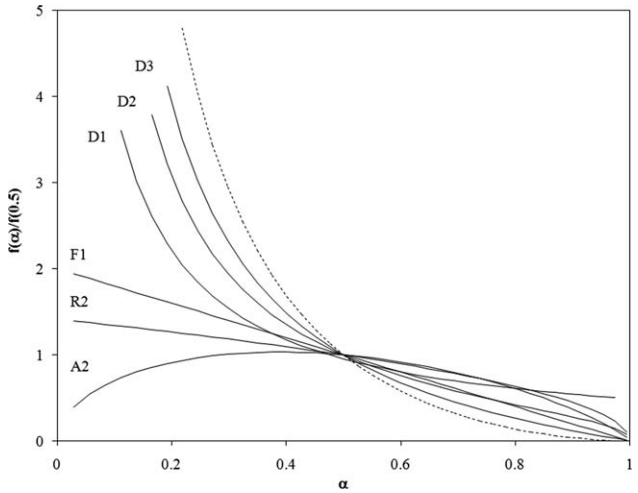

Figure 5. Comparison of $f(\alpha)$ normalized at $\alpha = 0.5$ $[f(\alpha)/f(0.5)]$ in the third stage between the least-squares best-fitted model with $n = 1.65$ and $m = -1.005$ based on eq. (6) for the cured polymer sample of native BMI/BTA (dashed line) and some of the ideal models shown in Table I (solid lines). Note that $\alpha = 0$ in the abscissae represents the start of the third stage and $\alpha = 1$ represents the end of the third stage.

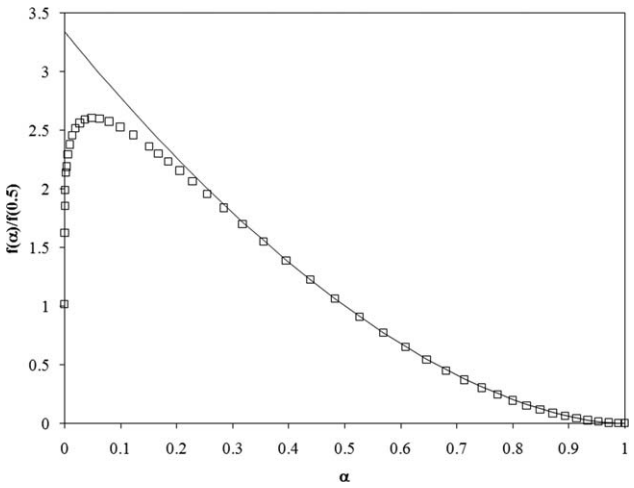

Figure 6. Comparison of $f(\alpha)$ normalized at $\alpha = 0.5$ [$f(\alpha)/f(0.5)$] in the first stage determined by the model-fitting method with different sets of n and m values for the cured polymer sample of S5: the least-squares best-fitted model with $n = 1.85$ and $m = 0.1$ (the discrete data points); the reference model with $n = 1.74$ and $m = 0$ (the continuous line). Note that $\alpha = 0$ in the abscissae represents the start of the first stage and $\alpha = 1$ represents the end of the first stage.

than that (336.12 ± 5.53 kJ mol^{-1}) obtained from model free method. Table I shows that the three diffusion models all have a value of m close to −1. This indicates that the thermal degradation process taking place in the third stage is a more complex process that includes the diffusion controlled reaction and other processes which have not been determined in this study yet.

As to the thermal degradation of the cured polymer sample of S5 in the first stage, the E_a and cA parameters obtained from the model-fitting method are 258.86 kJ mol^{-1} and 1.72 × 10^{21} min^{-1}, respectively, with the highest R^2 value of 0.995 for $n = 1.85$ and $m = 0.1$. In a manner similar to the kinetic analysis for the cured polymer sample of native BMI/BTA, the E_a and cA parameters associated with the first stage of the reference model are 258.56 kJ mol^{-1} and 1.34 × 10^{21} min^{-1}, respectively, with a R^2 value of 0.993 for $n = 1.74$ and $m = 0$. Figure 6 shows that the thermal degradation mechanism is most likely controlled by nucleation in the α range 0–0.2 in the first stage,[22] followed by the multimolecular decay law ($n = 1.74$) toward the end of stage 1.[19]

As aforementioned, E_a increases with increasing α in the second stage of the thermal degradation process for the cured polymer sample of S5 (Figure 2). This trend can be attributed to a rather complex degradation mechanism involved in this stage. The following equation involving two independent simultaneous processes can be used to successfully predict the complex thermal degradation data[23]:

$$\frac{d\alpha}{dt} = l_1 c_1 A_1 \exp\left(-\frac{E_{a1}}{RT}\right)(1-\alpha_1)^{n_1}\alpha_1^{m_1} + l_2 c_2 A_2 \exp\left(-\frac{E_{a2}}{RT}\right)(1-\alpha_2)^{n_2}\alpha_2^{m_2} \quad (7)$$

where the subscripts 1 and 2 refer to the first and second process, respectively, l_1 and l_2 represent the fractional contribution of the first and second process to the overall thermal degradation reaction. In addition, both the relationships $l_1 + l_2 = 1$ and $l_1\alpha_1 + l_2\alpha_2 = \alpha$ hold. It should be noted that the feasibility of this approach is verified only when the DTG data can be deconvoluted successfully. Unfortunately, an attempt to deconvolute the DTG data was made in this study, but in vain. To resolve this problem, it was assumed that the complex process involves two competitive parallel degradation reactions, as follows.

$$\frac{d\alpha}{dt} = k_1 f_1(\alpha) + k_2 f_2(\alpha) \quad (8)$$

After some mathematical manipulation, eq. (8) can be transformed into the following equation.

$$\ln\left[\frac{\frac{d\alpha}{dt} - A_1\exp\left(-\frac{E_{a1}}{RT}\right)f_1(\alpha)}{f_2(\alpha)}\right] = -\frac{E_{a2}}{RT} + \ln A_2 \quad (9)$$

where the subscripts 1 and 2 refer to the parallel reactions 1 and 2, respectively. At the very beginning of the complex process, the degradation mechanism approaches a single step reaction that only involves a single activation energy value.[25] Therefore, the values of E_{a1} and A_1 for reaction 1 were assumed to be equal to those (E_{a1} = 371.82 kJ mol^{-1} and $A_1 = 2.65 \times 10^{26}$ min^{-1}) determined at the start of the second stage via the model-free method. According to eq. (9), plotting the algebraic expression on the left hand side of eq. (9) versus $1/T$ data should result in a straight line with the least-squares best-fitted functions of $f_1(\alpha)$ and $f_2(\alpha)$. The validity of eq. (9) was confirmed by the satisfactory maximal value of R^2 through the evaluation of the available models (nucleation models, reaction order models, diffusion models, etc.). In this manner, the values of E_{a2} and A_2 for reaction 2 were determined from the slope and intercept of the least-squares best-fitted straight line. The corresponding kinetic parameters thus obtained are: E_{a2} = 443.42 kJ mol^{-1}, $A_2 = 2.51 \times 10^{30}$ min^{-1}, $f_1(\alpha) = (1-\alpha)^{2.4}$ and $f_2(\alpha) = 1.5[(1-\alpha)^{1/3}/(1-(1-\alpha)^{1/3}]$ (3-D diffusion) with the maximal $R^2 = 0.998$. It is also interesting to note that the E_{a2} value is very close to that (E_a = 445.15 kJ mol^{-1}) attained at the end of the second stage by using the model-free method. This result supports that eq. (9) proposed in this study can be used to effectively determine the kinetic parameters of the complex process without resort to the deconvolution technique. Nevertheless, such an approach is incapable of determining the fractional contribution of the individual process. In summary, the thermal degradation process of the cured polymer sample of S5 occurring in the second stage is primarily controlled by the simultaneous reaction order mechanism (n = 2.4) and 3-D diffusion mechanism.

Finally, for the cured polymer sample of S5, the parameters E_a and cA for the thermal degradation process involved in the third stage obtained from the model-fitting method are 335.20 kJ mol^{-1} and 2.38 × 10^{20} min^{-1}, respectively, with the highest R^2 of 0.997 for $n = 1.45$ and $m = -1$. Similar to the cured polymer sample of native BMI/BTA thermally degraded in the third stage, the complex degradation process also includes the diffusion-controlled reaction and other mechanisms.

CONCLUSIONS

Designed TG experiments were used to investigate the non-isothermal degradation kinetics of BMI/BTA [2/1 (mol/mol)] based polymers in the presence of HQ. Adding a small quantity (5 wt %) of HQ that effectively suppresses free radical polymerization to the BMI/BTA reaction system (denoted as S5) changed the polymerization mechanism and kinetics and, consequently, resulted in polymer products with different molecular structures as compared to the native BMI/BTA polymerization system. This then greatly increased the activation energy (E_a) of the thermal decomposition process and decreased the degradation rate constant, thereby leading to the enhanced thermal stability. The thermal degradation processes for both the cured polymer samples of native BMI/BTA and S5 exhibited three distinct stages. The kinetic parameters were attained via the model-fitting method. For the cured polymer sample of native BMI/BTA, in the first stage, the thermal degradation process was controlled by nucleation, followed by the multi-molecular decay law. In contrast, the reaction-order model adequately described the thermal degradation kinetics in the second stage. The complex processes characterized by the reaction model were shown to satisfactorily describe the thermal degradation behavior the third stage. As to the cured polymer sample of S5, the thermal degradation process in the first stage was controlled by nucleation, followed by the multi-molecular decay law. In contrast, the degradation process in the second stage was primarily governed by the simultaneous reaction order mechanism and 3-D diffusion mechanism. Similar to the native BMI/BTA counterpart, the complex processes involved in the third stage were adequately described by the reaction model. All the experimental results indicated that incorporation of 5 wt % HQ into the BMI/BTA based polymer exhibited the greatly improved thermal stability.

ACKNOWLEDGMENT

The financial support from National Science Council, Taiwan is gratefully acknowledged.

REFERENCES

1. Dix, L. R.; Ebdon, J. R.; Flint, N. J.; Hodge, P.; O'Dell, R. *Eur. Polym. J.* **1995**, *31*, 647.
2. Grenier-Loustalot, M. F.; Da Cunha, L. *Polymer* **1998**, *39*, 1799.
3. Shen, Z.; Schlup, J. R.; Fan, L. T. *J. Appl. Polym. Sci.* **1998**, *69*, 1019.
4. Zhang, X.; Du, F. S.; Li, Z. C.; Li, F. M. *Macromol. Rapid Commum.* **2001**, *22*, 983.
5. Liu, Y. L; Tsai, S. H.; Wu, C. S.; Jeng, R. J. *J. Polym. Sci. Part A: Polym. Chem.* **2004**, *42*, 5921.
6. Sava, M.; Grigoras, C. V.; *J. Macromol. Sci. Part A: Pure Appl. Chem.* **2005**, *42*, 1095.
7. Pan, J. P.; Shiau, G. Y.; Lin, S. S.; Chen, K. M. *J. Appl. Polym. Sci.* **1992**, *45*, 103.
8. Su, H. L.; Hsu, J. M.; Pan, J. P.; Wang, T. H.; Chern, C. S. *J. Appl. Polym. Sci.* **2010**, *117*, 596.
9. Dušek, K.; Matějka, L.; Špaček, P.; Winter, H. *Polymer* **1996**, *37*, 2233.
10. Su, H. L.; Hsu, J. M.; Pan, J. P.; Wang, T. H.; Yu, F. E.; Chern, C. S. *Polym. Eng. Sci.* **2011**, *51*, 1188.
11. Liu, X.; Chen, D.; Yang, X.; Lu. L.; Wang, X. *Eur. Polym. J.* **2000**, *36*, 2291.
12. Chern, C. S.; Su, H. L.; Hsu, J. M.; Pan, J. P.; Wang, T. H. *Plastic Research Online, Society of Plastics Engineering (SPE).* **2011**. DOI: 10.1002/spepro.003621.
13. Yu, F. E.; Hsu, J. M.; Pan, J. P.; Wang, T. H.; Chern, C. S. *Polym. Eng. Sci.* **2013**, *53*, 204.
14. Vyazovkin, S.; Burmham, A. K.; Criado, J. M.; Perez-Maqueda, L. A.; Popescu, C.; Sbirrazzuoli, N. *Thermochim. Acta* **2011**, *520*, 1.
15. Pham, Q. T.; Hsu, J. M.; Pan, J. P.; Wang, T. H.; Chern, C. S. *Polym. Int.* **2012**. DOI: 10.1002/pi.4390.
16. Lua, A. C.; Su, J. C. *Polym. Degrad. Stab.* **2006**, *91*, 144.
17. Salin, I. M.; Seferis, J. C. *J. Appl. Polym. Sci.* **1993**, *47*, 847.
18. Sun, J. T.; Huang, Y. D.; Gong, G. F.; Cao, H. L. *Polym. Degrad. Stab.* **2006**, *91*, 339.
19. Perez-Maqueda, L. A.; Criado, J. M.; Sanchez-Jimenez, P. E. *J. Phys. Chem. A* **2006**, *110*, 12456.
20. Vyazovkin, S.; Sbirrazzuoli, N. *Macromol. Rapid Commun.* **2006**, *27*, 1515.
21. Khawam, A.; Planagan, D. R. *J. Phys. Chem. B* **2006**, *110*, 17315.
22. Sestak, J.; Berggern, G. *Thermochim. Acta* **1971**, *3*, 1.
23. Sanchez-Jimenez, P. E.; Perez-Maqueda, L. A.; Perejon, A.; Criado, J. M. *J. Phys. Chem. C* **2012**, *116*, 11797.
24. Sanchez-Jimenez, P. E.; Perez-Maqueda, L. A.; Perejon, A.; Criado, J. M. *Polym. Degrad. Stab.* **2010**, *95*, 733.
25. Sbirrazzuoli, N.; Vincent, L.; Mija, A.; Guigo, N. *Chemom. Intell. Lab. Syst.* **2009**, *96*, 219.